Imaging system to assess objectively the optical density of the macular pigment *in vivo*

Andrew O'Brien,[1,2,*] Conor Leahy,[1,3] and Chris Dainty[1,4]

[1]Applied Optics Group, National University of Ireland, Galway, Ireland

[2]Currently at Phase Focus Limited, Sheffield Digital Campus, Sheffield S1 2BJ, UK

[3]Currently at Biomedical Engineering Department, University of California Davis, Davis, California 95616, USA

[4]Blackett Laboratory, Imperial College, London SW7 2BZ, UK

*Corresponding author: andrewobrien@gmail.com

Received 16 May 2013; accepted 27 June 2013;
posted 22 July 2013 (Doc. ID 189452); published 23 August 2013

This paper presents an optical system called MacPI, which implements a two-color reflectance technique in combination with various hardware and software tools to assess objectively the macular pigment (MP) optical density *in vivo*. The system consists of a bespoke optical design, a control architecture, driver electronics, a collection of image-processing techniques, and a graphical user interface. The deficiencies of the technique employed and the solutions implemented in the MacPI system to confront those inherent frailties are presented. An overview of the effective interpretation of the acquired data and the techniques employed by MacPI in the acquisition of that data is discussed. The result of a comparison trial with an alternative device is also presented. We suggest that appropriate design of the hardware and an efficient interpretation of the acquired data should produce a system capable of consistent, accurate, and rapid measurements, while retaining the distinction of ease of use, portability, comfort for the subject, and a design that is economic to produce. Its versatility should allow both for a clinical screening application and for further investigation and establishment of the physiological role of the MP in a laboratory-based environment.

OCIS codes: (100.0100) Image processing; (170.0110) Imaging systems; (330.4460) Ophthalmic optics and devices; (330.7310) Vision.

http://dx.doi.org/10.1364/AO.52.006201

1. Introduction

A. Overview of the Macular Pigment

Investigation of the macular pigment (MP) reveals an extensive history of study, dating back to Buzzi [1], who in 1782 documented a yellow color in the center of the retina. Various investigators hypothesized on the origin and function of the pigment [2–5]; however, it was not until 1945 that Wald provided a more accomplished account of this yellow pigment [6].

Wald established that the pigment absorbed light between the wavelengths 430 and 490 nm, with maximum absorption taking place at 465 nm. Wald also demonstrated that the absorption spectrum of the pigment was characteristic of that of the xanthophyll lutein (a dihydroxy carotenoid usually found in plants) and correctly concluded that the MP contained this carotenoid. Wald also noted that the spectrum of the pigment, extracted from human retinas, agreed quite well with the visual estimate of the MP derived from the differences in the log sensitivity of the peripheral and the foveal area of the retina. Further studies using more advanced analytic techniques reveal a more complete understanding of the nature of the pigment [7–10]. Lutein and zeaxanthin,

1559-128X/13/256201-12$15.00/0

the primary constitutes of the MP, are not synthesized within the body, consequently the MP is entirely supplied by dietary intake. Therefore, development of MP exclusively in primates may be explained by their dietary patterns. Meso-zeaxanthin has recently been hypothesized to be an equally important component of the MP [11].

It should be noted that the fundamental procedure of incorporation of the carotenoids into the retinal tissues is still relatively poorly understood. The exact chemical orientation of the MP within the retina is unknown. Some orientations do explain the entoptic phenomena of Haidinger's brushes (human eye's ability to perceive polarization) [12]. However, the pigment's location, within the Henle fiber layer, means it is ideally positioned to intercept light incident on the cone photoreceptors and reduce the risk of potential photic damage [13] to these important photosensitive cells. Figure 1 displays the absorption spectrum for the MP as measured by a number of independent groups. Carotenoids have well-known antioxidant properties [14], and this in combination with its location results in the pigment's ability to combat reactive oxygen intermediates produced in the macular region, and thus protect the cones from any consequent oxidative damage [15]. Due to the MP's ability to combat the risks of photic damage and oxidative damage, and therefore prevent any potential photoreceptor cell damage, it seems logical to propose an evolutionary development of MP to aid in the protection of this area of the retina. Due to this inferred protective role several groups have proposed that the MP may have a role in the protection of the retina against the development of age-related macular degeneration (AMD) [16,17], which is the leading cause of blindness in the western world. The pigment may also have a role beyond protection due to its ability to absorb blue light, which is highly scattered by the ocular optics [18]. This filtering ability may aid in improving visual performance due to the reduction in the influence of the scattered blue light and reduction of induced chromatic aberration [19,20] on any incident light on the cone photoreceptors. It is also important to note that the amount of blue-sensitive cone photoreceptors is far less than the green and red equivalents [21], which will also contribute to the subject's visual perception. An interesting question arises as to whether the number of blue cones is due to the presence of the pigment or whether the cone population evolved independent of the MP.

B. Techniques to Measure MP Optical Density *In Vivo*

In vivo measurement of the MP can be achieved by the objective techniques of reflectance [26,27], autofluorescence [26] and Raman spectroscopy [28,29], and the subjective techniques of heterochromatic flicker photometry [30–32] and color matching [22]. Associated with each of these techniques are various advantages and disadvantages that can be broadly categorized as consistency, accuracy and speed of measurement, complexity of device required, ease of use, and comfort for the patient. Measurement consistency and accuracy must be an imperative for any device pertaining to assessment and study of the MP optical density (MPOD) in a scientifically accepted manner. In addition to this fundamental necessity, a device that is rapid, easy to use, and comfortable for the patient should be an objective for any potential measurement system.

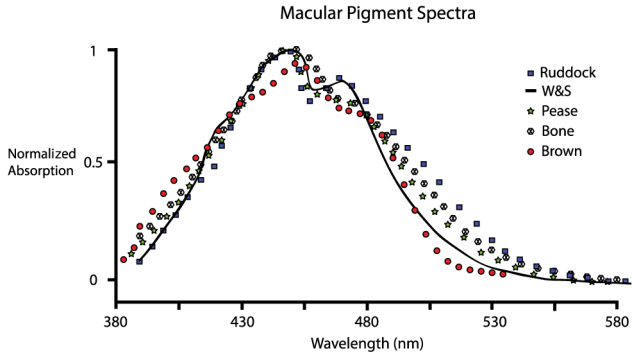

Fig. 1. Normalized absorption spectrum of the MP as measured by Ruddock [22], Wyszecki and Stiles [23], Pease *et al.* [24], Bone *et al.* [25], and Brown (taken from data in [26]).

The MacPI system measures the OD of the MP by implementing the objective technique of reflectance. This was the chosen technique because of its potential to significantly outperform subjective techniques in terms of accuracy, consistency, and speed of measurement. This potential for improvement in performance is due primarily to the removal of the complete reliance on the patient to provide the fundamental data from which to estimate the MPOD. Subjective devices may be amended to account for certain inaccuracies in the accumulation of data; for example, certain hardware amendments may be possible to confront ocular scatter, the Troxler effect [33], and edge effects due to fixation drift [34]. Further reduction in measurement error might be achieved by repeating the measurement task at the cost of total measurement time. However, some subjective data can be corrupted by factors that cannot be sufficiently appreciated and therefore appropriately accounted for. This includes patients' perceived perception, loss in data quality due to patient fatigue, and various other patient psychological and physical effects. Reflectance has the potential to outperform alternate objective techniques in terms of device complexity, ease of use, and overall cost of production.

All techniques have deficiencies in the acquisition of data. Therefore, in order to maximize the accuracy and consistency of the results obtained, those deficiencies must be confronted and accounted for in hardware and in the postprocessing of the data. The success of the reflectance technique is determined by appropriately interpreting the acquired data and providing tools in hardware to maximize the usefulness of the data and subsequently to appreciate and account for the potential aspects of the

technique that can detrimentally affect the quality of that data.

2. Description of the MacPI System

The MacPI system operates by analyzing reflected light from a blue and green illuminated retina. The blue light is maximally absorbed by the MP and green is minimally absorbed by the MP. This is achieved by custom-built hardware that provides adequate retinal images capable of providing information regarding the absorption of the pigment and in addition providing images that accommodate a method of accounting for ocular scatter. Figure 2 illustrates the layout of the optical setup.

The system is designed to obtain nonmydriatically four green ($\lambda_G = 535$ nm, $\Delta\lambda_G = \pm 30$ nm) and four blue ($\lambda_B = 460$ nm, $\Delta\lambda_B \pm 20$ nm) images over a 10° area on the retina. The illumination source is a custom-designed ring of four blue (Luxeon Rebel LXML-PB01-0040) and four green LEDs (Luxeon Rebel LXML-PM01-0100) mounted on a custom-designed heat sink. Figure 3 illustrates the method in which corneal reflections are avoided. The curvature of the cornea is utilized to redirect this unwanted reflected light out of the imaging arm. A measurement consists of four image sets, with each set containing one green and one blue measurement. An MPOD measurement is calculated for each blue–green image pair. An average reading is then calculated on the four individual measurement pairs. A dark frame is also obtained in order to reduce noise characteristics of the system. A saturation pulse is also presented to the patient in order to minimize the absorption by the cone photopigments. Total measurement time is approximately 1 s. The system behavior is fully controlled using an Arduino microcontroller, which can be programmed to output the appropriate waveform to control the electronic driver to respond to commands from the graphical user interface. This allows for individual LED brightness to be controlled via pulse width modulation and LED switching and camera triggering to be completely synchronized. Subject alignment is achieved both by mounting the system on an adjustable XYZ mount and providing a red switchable fixation target (visible over green and blue primary illumination light). The control of the fixation target is again dictated by the microcontroller.

Equation (1) displays the algorithm for transforming reflectance values (pixel values on CCD) to absorption values:

$$D_{\mathrm{mp}}(x,y) = \frac{0.5}{\kappa_{\mathrm{mp},G} - \kappa_{\mathrm{mp},B}} \left[\log_{10}\left(\frac{R_{P,G} - S_G}{\frac{R_{F,G}(x,y)}{U_G(x,y)} - S_G} \right) - \log_{10}\left(\frac{R_{P,B} - S_B}{\frac{R_{F,B}(x,y)}{U_B(x,y)} - S_B} \right) \right]. \quad (1)$$

The algorithm is based on Wald's original observations [6], which were expanded on by Delori *et al.* [26]. The reflectance values extracted are an array of pixel values within the macular region for both colors [$R_{F,G}(x,y)$ and $R_{F,B}(x,y)$], a peripheral reflectance value representing the parafoveal region for both

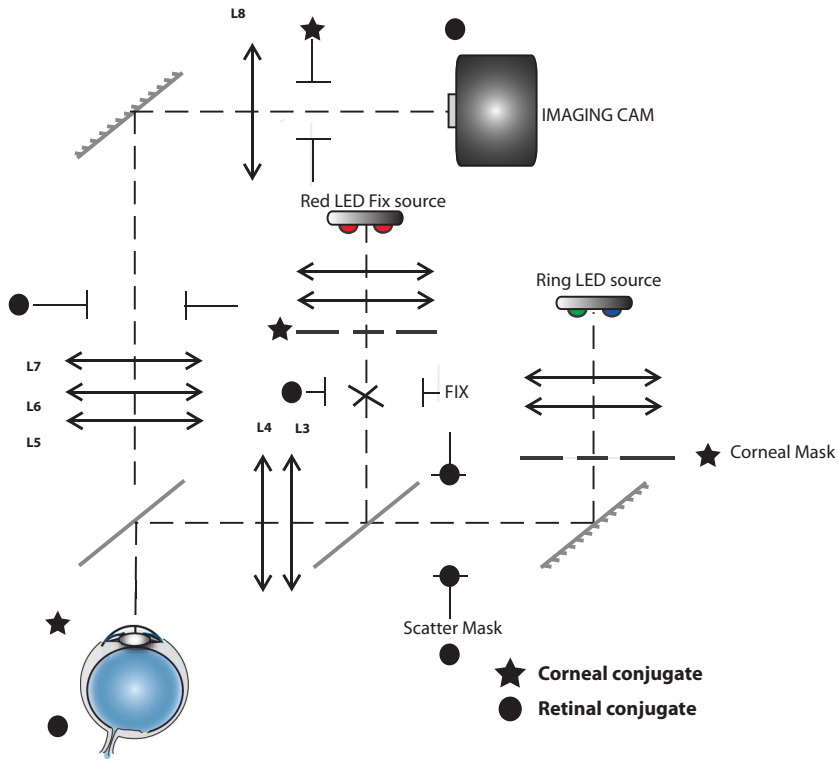

Fig. 2. Schematic of the optical layout for the measurement of MPOD. The device is mounted on an adjustable XYZ mount.

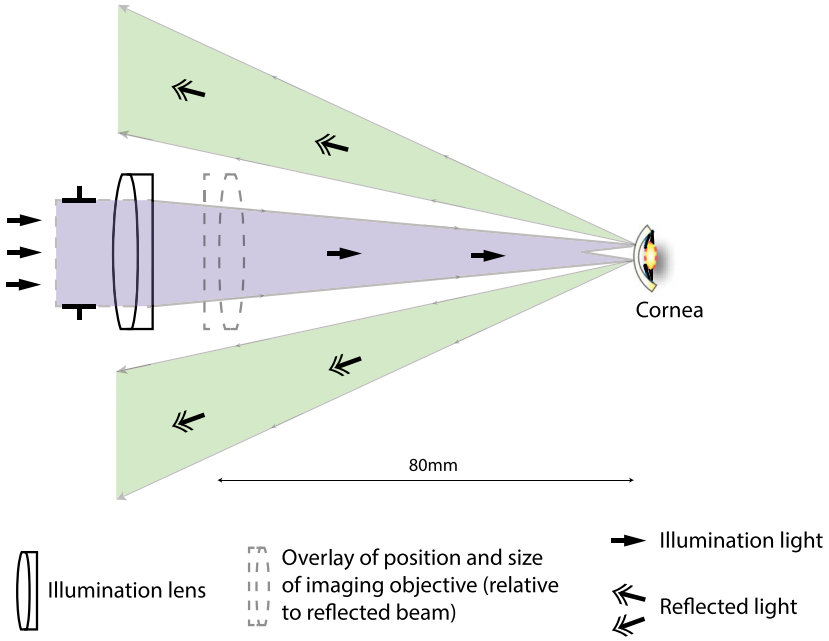

Fig. 3. Illustration demonstrating the utilization of the illumination light corneal reflex to avoid contamination of the retinal image.

colors ($R_{P,G}$ and $R_{P,B}$), a scatter compensation factor for both colors (S_G and S_B), and a correction surface to compensate for nonuniform illumination within the macular region for both colors [$U_G(x,y)$ and $U_B(x,y)$]. The extracted value [$D_{\mathrm{mp}}(x,y)$] is corrected for the illumination LEDs' spectral characteristics by means of the extinction coefficients ($\kappa_{\mathrm{mp},G}$ and $\kappa_{\mathrm{mp},B}$), with the 0.5 in the numerator accounting for the double-pass nature of the measurement. The accuracy and consistency in pigment extraction is determined by accurate and consistent calculation of each of these components. This is achieved in the MacPI system by a combination of hardware and software. The hardware provides images of sufficient retinal area, wavelength, bit depth, and resolution that the software can subsequently interpret and correct for known characteristics, in order to provide an accurate assessment of the MP distribution.

Figure 4 displays an illustration of the patient view, and a real green illuminated retina and blue illuminated retina. The macular region is circled in each image and the four scattering struts are clearly visible. The acquired images provide information on nonuniformities in illumination and induced ocular scatter that must be accounted for in order to accurately extract the pigment. The intensity values of the pixels in the blue and green image can be used to infer absorption information from the retina and consequently isolate information regarding the MP. The darker region visible in the center of the blue image illustrates the increased absorption in this region, due to the presence of the blue-absorbing MP. The following sections outline the procedures in accurately extracting the required information from this fundamental data in order to calculate the MPOD.

A. Macular Region Identification and Interimage Shift Determination

Inspecting Eq. (1), it is apparent that a dependable calculation of the MPOD is reliant on a direct comparison of the blue and the green image, or more particularly the direct comparison of corresponding features contained within the blue and green image.

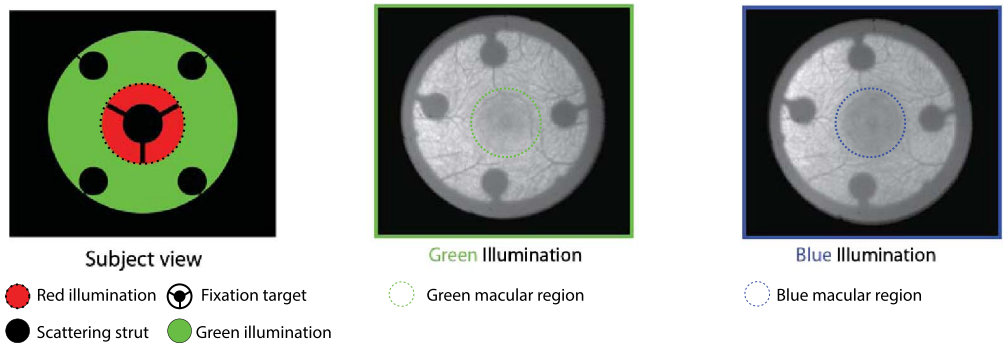

Fig. 4. Illustration of patient view looking into the MacPI system. Real images (green and blue) obtained from the MacPI system displaying macular regions and scattering struts.

Therefore, it is vital that when comparing features within the images, the identical retinal area of both images is selected. Subsequently, the information returned is due to spectral differences on the retina and not due to any spatial ambiguity. This is easily achieved with a static target, as the exact same Cartesian coordinates can be applied to both images; however, because this is an *in vivo* measurement, movement of the retina between image acquisitions is inevitable. Certain precautions may be implemented to suppress the extent of this eye movement, such as fast acquisition time, low-intensity illumination light, avoidance of alternate flashing of illumination source, and intermittent presentation of fixation target in between image acquisitions. However, a certain interimage displacement is expected and must be corrected for.

In order to accurately extract the MPOD, the macular region and the corresponding calibrating parafoveal region must be correctly defined for both colors. This process can be automated by utilizing an appropriately designed matched filter to locate the distinctive darkened reflectance pattern of the macula in the retinal image [35]. An inverted Gaussian function of the form

$$G(x,y) = \frac{d_c}{2}\left(1 - \frac{1}{2}e^{-\frac{x^2+y^2}{2\sigma^2}}\right) \tag{2}$$

was chosen as the matched filter kernel function, where d_c denotes the image bit depth and σ represents a tuning parameter. The size of the template was chosen depending on the camera binning settings. A fast normalized cross-correlation algorithm was then used to localize this template in the acquired retinal image [36]. The normalized cross correlation between an image $I(x,y)$ and the template G can be written as

$$R_{IG}(u,v) = \frac{\sum_{k,l}[I(k,l) - \langle I_G\rangle][G(u-k,v-l) - \langle G\rangle]}{\sqrt{\sum_{k,l}[I(k,l) - \langle I_G\rangle]^2 \sum_{k,l}[G(u-k,v-l) - \langle G\rangle]^2}}, \tag{3}$$

where $\langle I_G\rangle$ is the mean of the image in the region under the template. The location of the center of the macular region for a given image is then found by determining the location of the peak of the cross-correlation function. Once the center of the macular region is determined, the exact extent of the macular region is predefined by selection of the desired macular area.

Relative shifts between images within a particular image set were quantified by applying a Wiener filter-based algorithm within a specified region of interest to detect a local point spread function, using a method described by Fraser *et al.* [37]. The calculated relative shifts were used to register all images in a given set to the same coordinate system.

The macular localization algorithm was found to have better performance on the green images. This is primarily due to superior image quality in the green images because of the decreased amount of scatter induced by the ocular optics [18]. A green image from each image set was thus used to locate the macula, with the position of the macula within the blue image found indirectly using the image registration procedure. This proved to be far more successful in accurately identifying the macular region in each image set and ensuring that the exact same area of the retina is being assessed in each image set.

B. Parafoveal Reflectance Calculation

The parafoveal region is defined as the area peripheral to the defined macular region but excluding the additional image features, such as the scattering struts and field stop (see Fig. 5). The

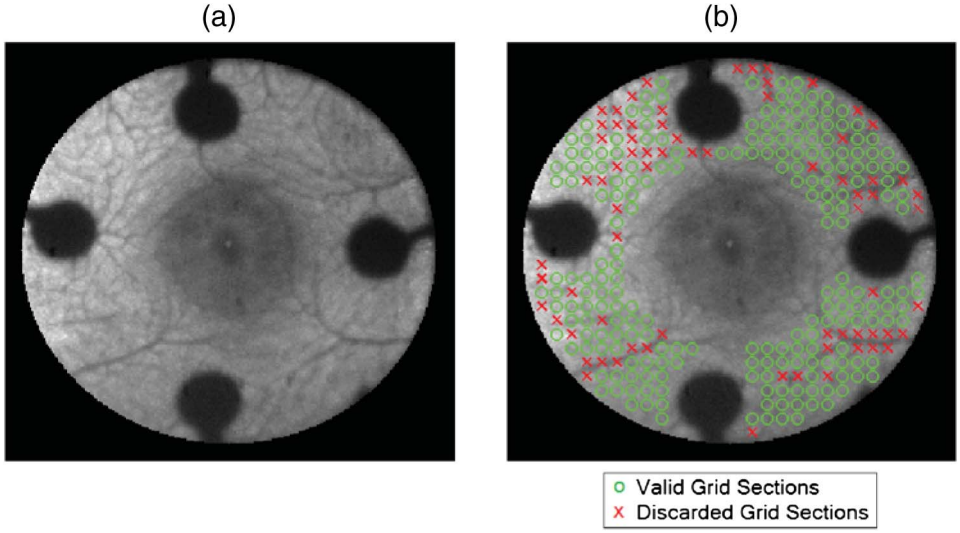

Fig. 5. (a) Typical image acquired under blue illumination. (b) Same image with overlay of grid section designations. Valid sections for the parafoveal calculation are determined by virtue of their relative structure content. Note that the macular and strut regions are excluded from this process, as they inherently contain structure.

parafoveal region is utilized to account for possible differences in illumination power between measurement wavelengths, as the parafoveal region represents an area of the retina where no MP is present. Accordingly, the differential absorption between the blue and green illumination light in the macula should not be present in the parafovea. Therefore, the parafoveal region is essentially employed as an estimate to calibrate the measurement procedure. Of course, there are other factors affecting reflection in the parafoveal region, such as melanin, blood vessels, ocular scatter, and penetration depth. This will return a false background measurement and consequently a corrupted calibration measurement. The primary contributor to this undesired intensity alternation is blood vessels (see Fig. 5, where primary parafoveal feature is the vascular tree). These features will cause a drastic underestimation of the parafoveal values and as such must be discounted from any calculation to determine the true "flat field" value.

MacPI utilizes a thresholding method based on structure content in order to exclude areas containing structure from the parafoveal reflectance calculation, similarly to Schweitzer *et al.* [38]. The software divides the retinal image into a grid of uniformly sized sections.

The values of entropy (H) for each grid section can then be used to compare the sections for the relative degree of structure present. If there is a lower degree of structure present in a particular grid section, a low entropy value is expected. Higher entropy values suggest there may be a blood vessel or other retinal feature or artifact present in that grid section. The lowest 75% of H values were deemed to correspond to regions of lowest structure; these grid sections were then regarded as "valid" choices for use in determining the parafoveal reflectance. Figure 5 shows a designation of grid sections computed for a typical image.

The macular and strut regions are excluded from this process, as they inherently contain structure. The mean pixel value of each valid grid section was computed. The parafoveal reflectance value was then found by gathering these mean values together and computing an overall median. The median average is chosen in order to exclude any outliers from the calculations that would skew the data. Outliers arise from either an entire grid location consisting of a vessel (low pixel reading) or flare light (high pixel reading).

C. Correction of Nonuniform Illumination

The retinal images are frequently corrupted by unwanted variations in intensity that occur due to general imperfections in the image illumination and acquisition process. These corruptions can originate from some individual retinal anomaly or misalignment during the acquisition process that can result in contaminating flare light. This inhomogeneous illumination across the retina can limit the useful information accessible within the acquired image. Specifically, this can lead to serious difficulties when extracting the true MPOD. Given that the spatial frequency content of the shading profile often overlaps with that of retinal features, retrospectively correcting for inhomogeneous illumination while maintaining the radiometric fidelity of the real data can be challenging. Retaining radiometric fidelity is vital, as a separate assessment of the illumination profile is calculated on each individual image so the subsequent direct comparison of intensity values of images must not be artificially altered by the correction process.

For each acquired image, MacPI attempts to recover an estimate of the true (i.e., shading-free) reflectance image $I_t(x,y)$. The true image is assumed to be a result of the interaction between a uniform illumination source and the object of interest. $I_t(x,y)$ cannot be measured directly and so must be inferred from the acquired image obtained using the (imperfect) optical system. This is referred to as the acquired or shaded image $I(x,y)$. The problem of correcting inhomogeneous illumination is therefore to obtain an estimate of $I_t(x,y)$ from $I(x,y)$. MacPI assumes that the inhomogeneous illumination is characterized by some smooth multiplicative function $U(x,y)$, and thus the shaded and shading-free images are related by

$$I(x,y) = U(x,y)I_t(x,y). \tag{4}$$

The problem of estimating $I_t(x,y)$ therefore reduces to finding a suitable estimate of $U(x,y)$ and then inverting the model. The estimate should be a smooth function, as shading effects are typically slow varying across the image [39].

The method of estimating $U(x,y)$ first necessitates removing from the image any prominent foreground features, such as the vascular structure, fovea, and optic disc. Pixels corresponding to retinal features are masked to yield an initial estimate $\hat{U}(x,y)$ of $U(x,y)$ that contains undefined values. These values are then estimated by obtaining an approximate solution of Laplace's equation $\nabla^2 U = 0$. This procedure is described in detail in a separate work [40]. The procedure results in providing image pairs where any potentially contaminating false variations in intensity profiles are corrected, while maintaining the integrity of the true reflectance values.

D. Scatter Compensation

Forward scattering induced in the illumination light by the eye can lead to a significant underestimation of the extracted MPOD. It is therefore necessary to account for the scatter in each acquired image. Delori *et al.* [26] employed a physical displacement of the illumination source to acquire a baseline measure of scattered light. Building on this and methods proposed by Ginis *et al.* [41], we make an on-line measurement of scattered light with the MacPI system by imaging a bespoke mask (scatter mask located in

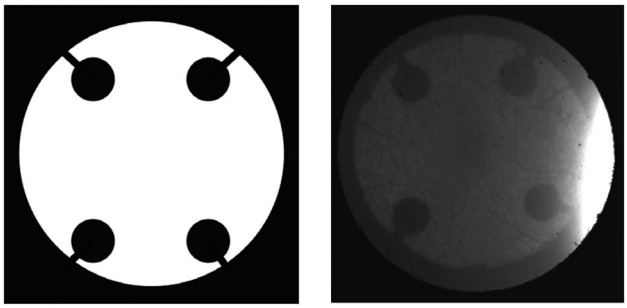

Fig. 6. (a) Illustration of the scatter mask utilized in the MacPI system and (b) example of contaminating of scatter data by flare light.

retinal conjugate of illumination arm) onto the retina and analyzing the image of this superimposed mask. Figure 6 illustrates the design of the scattering mask. The dimension of the mask is dependent on the magnification properties of the illumination relay optics. From the acquired images, MacPI computes a stray light equivalent quantity, denoted S_G and S_B. The first step in computing a value for S_G and S_B is to localize the strut regions within the image. The locations of these regions remain fixed as long as the optical system is not altered, and thus their positions can be stored as constants within the analysis software. If a precalibration of the imaging system is required (for reasons such as the subject having a large refractive error), the image of the struts formed at the sensor may be altered slightly. Therefore, it is desirable to automatically localize the positions of the struts for each measurement. This is achieved using a matched filter with a "top-hat" kernel function. The output of the filter will be a function whose local maxima give the position of the strut centers.

For each strut, a corresponding average intensity value must be computed. The average intensity of light incident on a circular region of the image plane is given by

$$\bar{I} = \frac{1}{\pi R^2} \iint_{(x^2+y^2)\le R} I(x,y)\mathrm{d}x\mathrm{d}y, \tag{5}$$

where $\bar{I}$ denotes the average light intensity on the sensor, $I(x,y)$ denotes the image intensity given by the CCD sensor, and R is the radius of the circular region. Assuming the struts are circular, an average intensity value can be obtained for each of the struts.

The stray light equivalent S_{eq} is assigned based on a weighted average of the strut intensity values. Each value is weighted by the reciprocal of the strut's geometric distance from the macular region. The weighting factor for a particular strut n is $w_n = 1/d_n$, where d_n is the Euclidean distance (in pixels) between the center of strut n and the center of the macular region. The value of S_{eq} is then given by

$$S_{\mathrm{eq}} = \frac{\sum_{k=1}^{M} w_k \bar{I}_k}{\sum_{k=1}^{N} w_k}, \tag{6}$$

where M is the total number of struts. MacPI also ensures that any contamination in the region of the struts is ignored. Contamination will arise from flare light, which will artificially raise the calculated pixel values within a particular strut. Consequently, the true scatter reflection value would be incorrect. To combat this a median average is calculated, or the operator has the choice to dismiss the contribution from any particular strut. Figure 6(b) illustrates an example of flare light artificially influencing the scatter strut values.

The method outlined above compensates the forward scatter induced in the illumination light by the system optics subsequent to the mask and the ocular optics (and vitreous) of the subject. The scatter induced by the system is negligible compared to the influence of the cornea and the lens. It should also be noted that any higher order scattering from the retinal layers cannot be distinguished using this technique.

3. Preliminary Results

The fundamental differences in the measurement technique and the returned measurement values for an objective device and a subjective device result in difficulty in performing an absolute comparison between the contrasting devices. The objective MacPI system returns a distribution of the pigment across the macular region (approximately 6° visual angle) from which a number of values are subsequently extrapolated. The subjective devices either return a single reading averaged over a sampled retinal area of 0.5° visual angle (M|POD from ZeaVision) or a distribution of discrete averaged retinal samples of 0.25°, 0.5°, and 1° (Densitometer from Macular Metrics). In order to compare the two measurement techniques it is important to correctly identify comparable metrics for the description of the MPOD. However, it must be stated that this is merely an aesthetic quality to fairly compare both devices, and as such it is imperative that a well-defined global metric for the description of MPOD is clearly defined in the future.

A. MacPI MPOD Metrics

For each MacPI measurement, three metrics of MPOD are automatically computed: peak value, average, and weighted average. The peak MPOD is simply the maximum value of D_{mp} within the defined area. The average is computed as the simple median of D_{mp}. A weighted average μ_w was also computed, using the formula

$$\mu_w = \frac{\iint_\Omega D_{\mathrm{mp}}(x,y)W(x,y)\mathrm{d}x\mathrm{d}y}{\iint_\Omega W(x,y)\mathrm{d}x\mathrm{d}y}, \tag{7}$$

where $W(x,y)$ is a simple 2D Gaussian weighting function and Ω is the prescribed extent of D_{mp}.

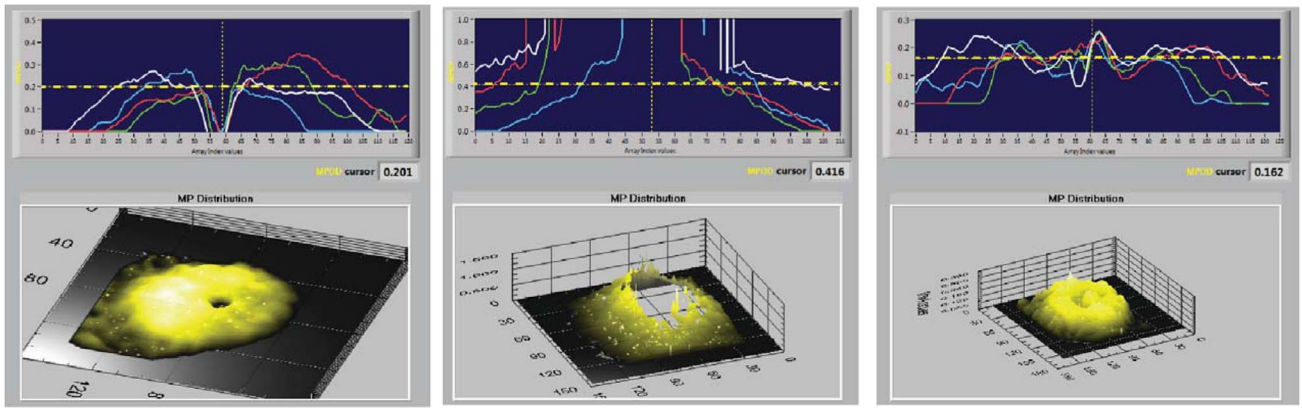

(a) (b) (c)

Fig. 7. Illustration of the implementation of the visual estimate. This figure illustrates (a) a false hole, (b) a false peak, and (c) a noisy profile. Each graphic is a screen grab from the MacPI software. The dashed line in the upper line profile plots represents the visual estimate of the MPOD.

The weighting adds emphasis to the most central part of the MP. This metric may be the most useful when comparing with data from the subjective instruments, which include MPOD readings at small central eccentricities [42].

The presence of noise within D_{mp} can significantly influence the computed metrics. For this reason, MacPI also offers an option to record an estimated value of MPOD based on a visual inspection of the result. Figure 7 displays three incidences where noise in the extracted profile results in false anomalies that may affect the automated extraction of the various metrics. In such cases the operator can adjust a horizontal bar over the 2D line profiles of the pigment distribution to extract the visual estimate metric. A sufficient method to filter out or to avoid the occurrences of these various anomalies in the MP distribution is currently under testing.

B. Variability of Measurement

The variability in measurement of the MacPI device was assessed by performing a number of repeat measurements on the same subject on the same day. The same procedure was also applied to a subjective device in order to compare the performance of both devices for that particular subject. In order to extend the evaluation of the repeatability an indirect comparison was performed, which allowed for a comparison with other subjective devices, across a greater number of subjects. This indirect comparison was possible by implementing the metric of the repeatability coefficient. Both comparisons are presented in the following sections.

1. *MacPI Consistency: A Direct Comparison*

The consistency of measurement was performed on a single trained subject and as such is only an indication of the potential performance of both devices. A series of 25 measurements was performed using the M|POD (ZeaVision) and using MacPI. The measurements were carried out on the same day with an adequate break (approximately 1 min) between each measurement. The subject was familiar with both devices. The quoted metric for MacPI is the weighted average. The total time for 25 measurements was 30 min for MacPI and 250 min for M|POD.

Figure 8 illustrates repeated MPOD measurements on both MacPI and M|POD. The MacPI average values have been normalized to the average subjective result, in order to obtain a more comparable representation of the variation in the measurement between the two devices. MacPI demonstrates more consistency in the measurement of the MP for this subject in this scenario. The low repeatability of the M|POD (ZeaVision) in a test retest scenario has also been commented on by Loughman *et al.* [43].

2. *Repeatability Coefficient: An Indirect Comparison*

For the measurement of MPOD, repeatability has generally been assessed using a method proposed by Bland [44], which relies on two key assumptions. First, the data must be normally distributed and second, the variance of repeat measurements is the same for every subject. Given at least two measurements for each subject measured, the intersession repeatability is then given by 1.96 times the standard deviation of mean differences between the repeated sets of data. This method lends itself well to a clinical environment, as it can be applied when there is a very limited number of measurements (as little as two) available for each subject [43,45,46]. Applying this method to the MacPI device, five repeat measurements were performed on 18 young, healthy subjects. The obtained repeatability figure is compared in Table 1 to that of other instruments in published studies.

This method of extrapolating the repeatability coefficient of a measurement device is convenient for devices where the measurement time is excessive and therefore restrictive in the number of measurements that can be performed. The advantage of this

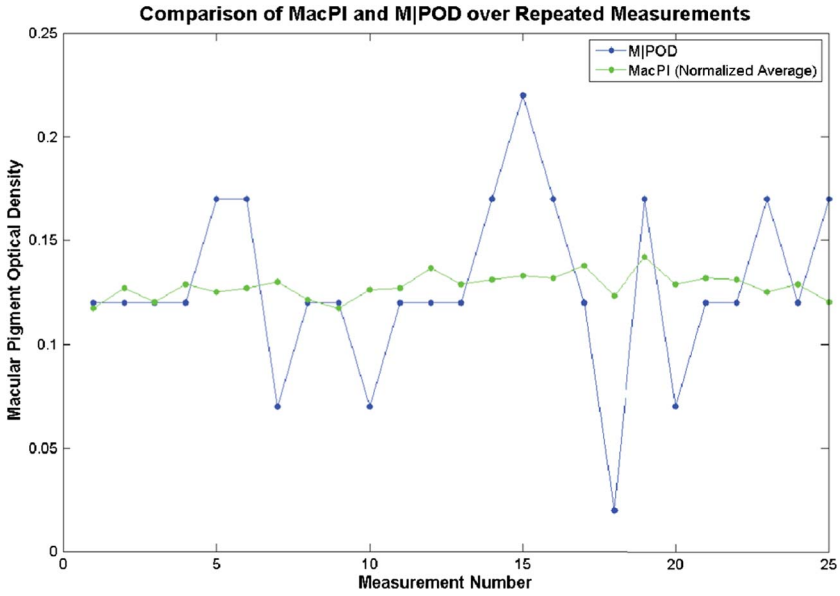

Fig. 8. Repeated measurements using MacPI and the M|POD (ZeaVision) devices.

procedure is that only two measurements are performed, which greatly reduces overall time for the collection of data. However, as mentioned previously, the accurate extraction of the repeatability coefficient from this limited data sample depends on the assumption that the overall data population is normally distributed and there is uniform variance across all subjects. In other words, the assumption is that all subjects will perform equally well. Examining this assumption in more detail one disputable expectation is that subjects with low pigment levels will perform to the same accuracy and competency as subjects with higher pigment levels. This appears to be an erroneous premise, as a greater contrast in visual perception, between the green and blue illuminated targets, will exist for subjects with higher MPOD than those with lower MPOD, and therefore performing the required subjective task may be easier for the subjective and consequently more repeatable. In addition various other factors, both physical and psychological, will ensure that not all subjects will perform equally for every measurement. One solution is to perform a greater number of measurements and quote the standard deviation of the measurement as an indicator of the system's repeatability, but of course this is restrictive due to the time required to accumulate an acceptable cohort of data.

Table 1. Coefficient of Repeatability for Three Devices[a]

Instrument	Repeatability Coefficient
Densitometer (Macular Metrics)	0.19–0.21 [46]; 0.11–0.12 [43]
M|POD (MPS 9000)	0.28–0.33 [45]; 0.18–0.21 [43]; 0.02 [47]
MacPI	0.03

[a]The M|POD and Densitometer results are taken from the cited literature.

The performance of objective devices will also differ depending on the subject under examination. The limitation in dynamic range of the detector will result in less contrast for subjects with lower pigment levels and, as with the subjective devices, the assumption of a normal population distribution and uniform variance of the data will be challenged. The difference in quality for subjects with inferior ocular optics will also affect the quality of data returned. However, due to the quick measurement time for objective devices, it is far more feasible to perform a large number of measurements on the MacPI device than on the subjective devices. Therefore, it is far more feasible to extract the standard deviation of the measurement population and achieve a far more dependable indication of the repeatability of the system.

A dependable method of assessing repeatability is vital for any device pertaining to measurement of the MPOD. Without an accurate measurement of the repeatability of the device, it is difficult for the operator to conclude whether alterations in pigment levels are due to measurement noise of the procedure or due to true changes in the pigment level of a particular subject.

C. Device Correlation

As mentioned in a previous section both devices employ different techniques to assess the MP level, and as such comparable metrics must be decided on. The goal of the authors is not to repeat the exact results obtained from a different instrument but to demonstrate acceptable correlation between these comparable metrics from both devices.

1. Choice of Comparable Metrics

The subjective device used in this correlation test is the Densitometer from Macular Metrics. In order to

compare the two devices a comparable metric must be chosen. The various metrics returned from the subjective device represent the MPOD at a number of retinal eccentricities, namely 0.25°, 0.5°, and 1°. From these values an overall average and a centrally weighted average can be calculated. It can be difficult to maintain accurate fixation throughout the subjective measurement, which can lead to a smearing of the MPOD across the various metrics. This means that to take just the central value of 0.25° may lead to an inaccurate representation of the MPOD for that subject. Therefore, when searching for comparable metrics between this subjective measurement and the objective measurement, the logical choice is to compare a weighted central average for both devices.

D. Correlation Result

The MPOD was measured for 42 subjects on both the MacPI system and the Densitometer. The Macular Metrics device was the research version of the commercially available Densitometer, which has the capability of measuring the pigment at several eccentricities. The Densitometer device was operated by a researcher from the School of Optometry from Dublin Institute of Technology (DIT).

The subjects were 42 young, healthy adults with generally good ocular condition. The MPOD for each subject was obtained using both devices. The subjective measurements were calculated at a number of discrete locations and a distribution estimate was obtained. MacPI returned the *weighted average* metric and a *visual estimate* metric was also noted. Figure 9 displays the correlation for both MacPI metrics with that of the Densitometer results. As expected the highest correlation is found between the Densitometer's *central average* metric and both metrics returned by MacPI. Higher correlation values are found for the visual estimate over the weighted average metric between all Densitometer results. This is expected, as the visual estimate corrects for observed defects in the pigment distribution that the software has failed to account for.

The level of correlation does suggest that both devices are attempting to obtain an assessment of a similar feature from each subject. The difficulty is concluding which technique is returning a better estimate of the MPOD and what actual meaning to infer from the correlation results. Further amendments to the MacPI system may return a better estimate of the MPOD. This includes improved hardware and software techniques, improved scatter compensation, and a full correction for spectral discrepancies in the parafoveal region.

4. Discussion

The primary goal of this paper is to present the most appropriate technique, and associated hardware and software tools, for the measurement of the MPOD *in vivo*. The MacPI system is not a commercial entity but rather a research device, one that accommodates the implementation of the proposed reflectance technique and allows for the demonstration of the supplementary tools for the extraction of the MPOD distribution.

The objective reflectance technique, in combination with the associated tools, was found to demonstrate superior repeatability and greater accuracy than the subjective alternatives, while also exhibiting the ability to obtain a measurement in a more rapid and straightforward manner. The argument presented for this improved performance is primarily due to the removal of the dependence on a subjective interpretation of the measurement in order to extrapolate the result. The limitation in the subjective techniques to fully correct for various physical and psychological effects of the measurement task will always ensure an inferior performance. The reflectance technique has inherent limitations, but these potential negative factors can be quantified and accounted for in a far more effective manner. Consequently the potential of the reflectance technique depends on adequately recognizing the provenance of these contaminating sources and appropriately correcting for such. The success of the technique is therefore reliant on effective hardware

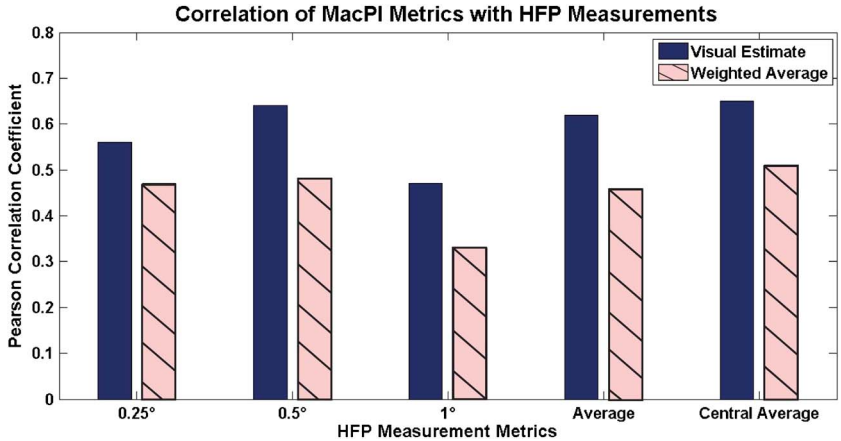

Fig. 9. Intercorrelation of Densitometer results.

and software design and not on the aptitude and dexterity of each subject under measurement.

The problem of selecting an appropriate metric to describe the MPOD distribution is also presented. Providing a metric to simplify the 2D surface profile of MPOD distribution into a single number would be desirable to aid clinical assessment; however, identifying the best-suited metric for the purpose is somewhat nontrivial. In reflectometry studies, peak and average quantities have been given, while psychophysical measurements often tend to supply MPOD at a fixed range of eccentricities. The additional problem arises of which metric from the different techniques to utilize when performing a correlation test. For the reflectance technique, the potential accuracy of the MP distribution is ultimately limited by the resolution and dynamic range of the imaging system. The subjective technique can also return a distribution, but this is limited by the sampling area of each retinal eccentricity and the ability of the subject in maintaining correct fixation, ensuring the correct area of the retina is sampled for all repeated measurements. Therefore, smearing of the different sample areas of the subjective distribution can manifest, and misrepresentation of the pigment distribution can arise. In addition the subjective method assumes a spatial symmetry to the pigment distribution that may not be the case. It is possible that the most suitable metric may be that, which correlates best with visual assessment of the full 2D MPOD spatial profile, when observed by an experienced operator. In comparing the subjective and objective devices a weighted average of each distribution was utilized. There was a certain correlation observed that suggests that both devices are measuring a similar aspect of the retina; however, a higher correlation can not be expected due to the inherent differences and performances of both techniques.

Accurate assessment of the MPOD *in vivo* is integral in competently establishing the evolutionary role of this yellow pigment. A commercial opportunity in the measurement of the MPOD may also emerge; however, it is morally imperative that some authentic and constructive information can be inferred from an accurate assessment of the pigment. The characteristics of the MP do suggest that the pigment serves a protective role against both photic and oxidative damage. This damage is cumulative and over a lifetime can result in meaningful damage. Age-related diseases are a growing public health concern due to a significant portion of the population now living longer than ever before. Among the elderly population within first world countries, the leading liability to their sustained vision is that of AMD. The underlying pathogenesis of this debilitating disease is still not fully understood, and consequently the treatment options, once the disease has established itself, are limited. Therefore, the key to combating the disease is early detection or prevention. The location of the pigment and its inferred protective role can make it very tempting to conclude that the pigment plays a role in protecting the retina against AMD. In addition, several epidemiological studies have associated frequent consumption of foods containing lutein and zeaxanthin, and high plasma levels of zeaxanthin and lutein, with a reduction in risk for AMD [16,17]. However, the direct link between MPOD levels and AMD is not established and further studies are essential. The lower pigment levels may be an overall indicator and consequence in deterioration in general health of a subject rather than a factor directly contributing to the development of AMD. As such the MPOD levels may be utilized as a risk indicator rather than a risk factor in relation to the development of AMD.

5. Conclusion

The measurement of the MPOD is a physics problem and as such successful assessment of the pigment requires an appreciation of the technique employed and appropriate measures to confront those inherent problems associated with the chosen technique. Further investigation of the MPOD requires that a dependable device is used in the measurement of the pigment. The quality of any instrument pertaining to measurement of the MPOD *in vivo* will depend on the strategy and processes implemented to account for these sources of error. It is imperative that any device pertaining to investigation and further study of the role of the MPOD must perform to a much higher standard than the subjective devices.

The authors thank Science Foundation Ireland and Enterprise Ireland for their support of this research. The authors also thank Dr. James Loughman and his colleagues at DIT for their help with obtaining the subjective results.

References

1. F. Buzzi, "Nuove sperienze fatte sulli occhio umano," Opuscoli Scetti Sulle Scienze e Sulle Arti **5**, (1782).
2. J. C. Maxwell, "On the unequal sensibility of the Foramen Centrale to light of different colours," Report of the British Association, 1856.
3. M. Schultze, "Uber den gelben Fleck der Retina, seinen Einflussauf normales Sehen und auf FarbenBlindheit," (On the yellow spot of the retina: its influence on normal vision and on colour blindness), (Von Cohen, 1866), pp. 1–5.
4. S. Soemmering, "De foramina centrali limbo luteo cincto retinae humanae," Comment Soc Reg Sci Goetting **13** (1799).
5. E. Home, "An account of the orifice in the retina of the human eye, discovered by Professor Soemmering: to which are added proofs of this appearance being extended to the eyes of other animals," Philos. Trans. R. Soc. London **2** (1798).
6. G. Wald, "Human vision and the spectrum," Science **101**, 653–658 (1945).
7. R. A. Bone, J. T. Landrum, L. Fernandez, and S. L. Taris, "Analysis of the macular pigment by HPLC: retinal distribution and age study," Invest. Ophthalmol. Visual Sci. **29**, 843–849 (1988).
8. R. A. Bone, J. T. Landrum, G. W. Hime, A. Cains, and J. Zamor, "Stereochemistry of the Human Macular Carotenoids," Invest. Ophthalmol. Visual Sci. **34**, 2033–2040 (1993).
9. F. Khachik, F. F. de Moura, D. Y. Zhao, C. P. Aebischer, and P. S. Bernstein, "Transformations of selected carotenoids in plasma, liver, and ocular tissues of humans and in nonprimate animal models," Invest. Ophthalmol. Visual Sci. **43**, 3383–3392 (2002).

10. O. Sommerburg, J. E. Keunen, A. C. Bird, and F. J. Kuijk, "Fruit and vegetables that are sources for lutein and zeaxanthin: the macular pigment in human eyes," Br. J. Ophthalmol. **82**, 907–910 (1998).
11. J. T. Landrum and R. A. Bone, "Lutein, zeaxanthin, and the macular pigment," Arch. Biochem. Biophys. **385**, 28–40 (2001).
12. R. A. Bone and J. T. Landrum, "Macular pigment in Henle fiber membranes: a model for Haidinger's brushes," Vis. Res. **24**, 103–108 (1984).
13. W. T. Ham, Jr., J. J. Ruffolo, Jr., H. A. Mueller, A. M. Clarke, and M. E. Moon, "Histologic analysis of photochemical lesions produced in rhesus retina by short-wavelength light," Invest. Ophthalmol. Visual Sci. **17**, 1029–1035 (1978).
14. W. Stahl and H. Sies, "Antioxidant activity of carotenoids," Mol. Aspects Med. **24**, 345–351 (2003).
15. F. Khachik, P. S. Bernstein, and D. L. Garland, "Identification of lutein and zeaxanthin oxidation products in human and monkey retinas," Invest. Ophthalmol. Visual Sci. **38**, 1802–1811 (1997).
16. J. T. Landrum, R. A. Bone, and M. D. Kilburn, "The macular pigment: a possible role in protection from age-related macular degeneration," in Vol. **38** of *Advances in Pharmacology*, H. Sies, ed. (Academic, 1996), pp. 537–556.
17. J. M. Seddon, U. A. Ajani, R. D. Sperduto, R. Hiller, N. Blair, T. C. Burton, M. D. Farber, E. S. Gragoudas, J. Haller, D. T. Miller, L. A. Yannuzzi, and W. Willett, "Dietary carotenoids, vitamins A, C and E and advanced age-related macular degeneration," J. Am. Med. Assoc. **272**, 1413–1420 (1994).
18. J. E. Coppens, L. Franssen, and T. J. T. P. van den Berg, "Wavelength dependence of intraocular straylight," Exp. Eye Res. **82**, 688–692 (2006).
19. J. M. Stringham and B. R. Hammond, "Macular pigment and visual performance under glare conditions," Optom. Vis. Sci. **85**, 82–88 (2008).
20. J. Loughman, M. Akkali, S. Beatty, G. Scanlon, P. Davison, V. O'Dwyer, T. Cantwell, P. Major, J. Stack, and J. Nolan, "The relationship between macular pigment and visual performance," Vis. Res. **50**, 1249–1256 (2010).
21. A. Roorda and D. R. Williams, "The arrangement of the three cone classes in the living human eye," Nature **397**, 520–522 (1999).
22. K. Ruddock, "Evidence for macular pigmentation from colour matching data," Vis. Res. **3**, 417–429 (1963).
23. G. Wyszecki and W. S. Stiles, *Colour Science: Concepts and Methods, Quantitive Data and Formulae*, 2nd ed. (Wiley, 1982).
24. P. L. Pease, A. J. Adams, and E. Nuccio, "Optical density of human macular pigment," Vis. Res. **27**, 705–710 (1987).
25. R. A. Bone, J. T. Landrum, and A. Cains, "Optical density spectra of the macular pigment in vivo and in vitro," Vis. Res. **32**, 105–110 (1992).
26. F. C. Delori, D. G. Goger, B. R. Hammond, D. M. Snodderly, and S. A. Burns, "Macular pigment density measured by autofluorescence spectrometry: comparison with reflectometry and heterochromatic flcker photometry," J. Opt. Soc. Am. A **18**, 1212–1230 (2001).
27. T. J. M. Berendschot and D. van Norren, "Objective determination of the macular pigment optical density using fundus reflectance spectroscopy," Arch. Biochem. Biophys. **430**, 149–155 (2004).
28. W. Gellermann, I. V. Ermakov, R. W. McClane, and P. S. Bernstein, "Raman imaging of human macular pigments," Opt. Lett. **27**, 833–835 (2002).
29. W. Gellermann, I. V. Ermakov, R. W. McClane, and P. S. Bernstein, "In vivo resonant Raman measurement of macular carotenoid pigments in the young and aging human retina," J. Opt. Soc. Am. A **19**, 1172–1180 (2002).
30. R. L. P. van der Veen, T. T. J. M. Berendschot, M. Makridaki, F. Hendrikse, D. Carden, and I. J. Murray, "Correspondence between retinal reflectometry and a flicker-based technique in the measurement of macular pigment spatial profiles," J. Biomed. Opt. **14**, 064046 (2009).
31. B. R. Wooten, B. R. Hammond, Jr., R. I. Land, and D. M. Snodderly, "A practical method for measuring macular pigment optical density," Invest. Ophthalmol. Visual Sci. **40**, 2481–2489 (1999).
32. J. Mellerio, S. Ahmadi-Lari, F. J. G. M. van Kuijk, D. Pauleikhoff, A. C. Bird, and J. Marshall, "A portable instrument for measuring macular pigment with central fixation," Curr. Eye Res. **25**, 37–47 (2002).
33. L. Lou, "Selective peripheral fading: evidence for inhibitory sensory effect of attention," Perception **28**, 519–526 (1999).
34. R. A. Bone, J. T. Landrum, and J. C. Gibert, "Macular pigment and the edge hypothesis of flicker photometry," Vis. Res **44**, 3045–3051 (2004).
35. C. S. Inthanayothin, J. F. Boyce, H. L. Cook, and T. H. Williamson, "Automated localization of the optic disc, fovea, and retinal blood vessels from digital color fundus images," Br. J. Ophthalmol. **83**, 902–910 (1999).
36. J. P. Lewis, "Fast template matching," in *Vision Interface 95* (Canadian Image Processing and Pattern Recognition Society, 1995), pp. 120–123.
37. D. Fraser, A. J. Lambert, and M. R. S. Jahromi, "Position-varying tip-tilt estimation and region-of-interest PSF derivation by Wiener filter," Proc. SPIE **5562**, 50–57 (2004).
38. D. Schweitzer, S. Jentsch, J. Dawczynski, M. Hammer, U. E. K. Wolf-Schnurrbusch, and S. Wolf, "Simple and objective method for routine detection of the macular pigment xanthophyll," J. Biomed. Opt. **15**, 061714 (2010).
39. D. Tomaževiĉ, B. Likar, and F. Pernuš, "Comparative evaluation of retrospective shading correction methods," J. Microsc. **208**, 212–223 (2002).
40. C. Leahy, A. O'Brien, and C. Dainty, "Illumination correction of retinal images using Laplace interpolation," Appl. Opt. **51**, 8383–8389 (2012).
41. H. Ginis, I. Pentari, D. De Brouwere, D. Bouzoukis, I. Naoumidi, and I. Pallikaris, "Narrow angle light scatter in rabbit corneas after excimer laser surface ablation," Ophthalmic Physiolog. Opt. **29**, 357–362 (2009).
42. B. R. Hammond, Jr., B. R. Wooten, and D. M. Snodderly, "Individual variations in the spatial profile of human macular pigment," J. Opt. Soc. Am. A **14**, 1187–1196 (1997).
43. J. Loughman, G. Scanlon, J. M. Nolan, V. O'Dwyer, and S. Beatty, "An evaluation of a novel instrument for measuring macular pigment optical density: the MPS 9000," Acta Ophthalm. **90**, e90–e97 (2012).
44. M. Bland, *An Introduction to Medical Statistics* (Oxford University, 2000).
45. H. Bartlett, L. Stainer, S. Singh, F. Esperjesi, and O. Howells, "Clinical evaluation of the MPS 9000 Macular Pigment Screener," Br. J. Ophthalmol. **94**, 753–756 (2010).
46. D. M. Snodderly, J. A. Mares, B. R. Wooten, L. Oxton, M. Gruber, and T. Ficek, "Macular pigment measurement by heterochromatic flicker photometry in older subjects: the carotenoids and age-related eye disease study," Invest. Ophthalmol. Visual Sci. **45**, 531–538 (2004).
47. R. L. P. van der Veen, T. T. J. M. Berendschot, F. Hendrikse, D. Carden, M. Makridaki, and I. J. Murray, "A new desktop instrument for measuring macular pigment optical density based on a novel technique for setting flicker thresholds," Ophthalmic Physiolog. Opt. **29**, 127–137 (2009).